Angewandte Chemie
Eine Zeitschrift der Gesellschaft Deutscher Chemiker

Supporting Information

Wavelength-Orthogonal Stiffening of Hydrogel Networks with Visible Light

V. X. Truong, J. Bachmann, A.-N. Unterreiner, J. P. Blinco, C. Barner-Kowollik**

Table of Contents

1. Experimental Procedures

1.1. Materials

Solvents (CH_2Cl_2, diethyl ether, petroleum ether, acetone, tetrahydrofuran, and methanol) were purchased from VWR in HPLC grade. 8-arm PEG20k-OH was purchased from Jenkem Tech, USA. 8-arm PEG$(NH_2)_8$ was synthesised from 8-arm PEG20k-OH according to a previously published procedure with a degree of conversion from -OH to -NH_2 group of 98%,[2] 3-(pyren-1-yl)acrylate-N-hydroxysuccinimide was prepared according to a previously published procedure.[3] All other chemicals were purchased from Sigma-Aldrich in the highest available purity and used as received.

Glassware for synthesis was first treated in a base bath (KOH in isopropanol 2 M) overnight, rinsed with water, subjected to second washing in a dishwashing machine, and dried in an oven at 70 °C for 6-12 h.

Thin-layer chromatography (TLC) was performed on silica gel 60 F254 alumina sheets (Merck) and visualized by UV light or potassium permanganate solution. Column chromatography was run on silica gel 60 (0.04-0.06 mm, 230-400 mesh ASTM, Merck).

Aqueous solutions of H_2O with different pH values were generated by subsequent dilution of water with 32% hydrochloric acid (Ajax Finechem, Analytical grade) or $NaHCO_3$ (Ajax Finechem, AR grade). The final pH values were recorded with an AQUAPHZ Rev. 3.1 (TPS, Australia) pH sensor after an equilibration period of 5 min. The pH sensor was calibrated against GB4 (pH=4.00) and GB7 (pH=7.01) solutions (TPS, Australia) by linear regression prior to usage.

1.2. Characterization

Nuclear Magnetic Resonance (NMR) Spectroscopy

NMR spectra a were recorded on a Bruker Avance III 600 MHz with a 5 mm broadband auto-tuneable probe with Z-gradients at 293 K. Chemical shifts are reported as δ in parts per million (ppm) and referenced to the chemical shift of the residual solvent resonances (CDCl3 δ = 7.26 ppm; DMSO-d6, δ = 2.5 ppm), couplings are shown as d: doublet, t: triplet, m: multiplet and bs: broad singlet. Polymer samples were prepared at a concentration of 20 mg mL-1. In most spectra, traces of water appear as a broad singlet close to 1.5-2.5 ppm. NMR spectra were processed using the MestReNova software suite.

Size Exclusion Chromatography (SEC)

SEC measurements were conducted on a PSS SECurity[4] system consisting of a PSS SECurity Degasser, PSS SECurity TCC6000 Column Oven (35 °C), PSS SDV Column Set (8·150 mm 5 µm Precolumn, 8·300 mm 5 µm Analytical Columns, 100000 Å, 1000 Å and 100 Å) and an Agilent 1260 Infinity Isocratic Pump, Agilent 1260 Infinity Standard Autosampler, Agilent 1260 Infinity Diode Array and Multiple Wavelength Detector (A: 254 nm, B: 360 nm), Agilent 1260 Infinity Refractive Index Detector (35 °C). HPLC grade THF, stabilized with BHT, is used as eluent at a flow rate of 1 mL·min-1. Narrow disperse linear poly(styrene) (Mn: 266 g·mol-1 to 2.52·106 g·mol-1) and poly(methyl methacrylate) (Mn: 202 g·mol-1 to 2.2·106 g·mol-1) standards (PSS ReadyCal) were used as calibrants. All samples were passed over 0.22 µm PTFE membrane filters. Molecular weight and dispersity analysis was performed in PSS WinGPC UniChrom software (version 8.2).

SEC Coupled to Electrospray Ionization (ESI)-Mass Spectrometry (MS)

SEC-ESI-MS spectra were recorded on a Q Exactive Plus (Orbitrap) mass spectrometer (Thermo Fisher Scientific, San Jose, CA, USA) equipped with an HESI II probe. The instrument was calibrated in the m/z range 74-1822 using premixed calibration solutions (Thermo Scientific) and for the high mass mode in the m/z range of 600-8000 using ammonium hexafluorophosphate solution. A constant spray voltage of 3.5 kV, a dimensionless sheath gas and a dimensionless auxiliary gas flow rate of 10 and 0 were applied, respectively. The capillary temperature was set to 320 °C, the S-lens RF level was set to 150 and the aux gas heater temperature was set to 125 °C. The Q Exactive was coupled to an UltiMate 3000 UHPLC System (Dionex, Sunnyvale, CA, USA) consisting of a pump (LPG 3400SD), autosampler (WPS 3000TSL), and a temperature-controlled column department (TCC 3000). Separation was performed on two mixed bed size exclusion chromatography columns (Agilent, Mesopore 250 × 4.6 mm, particle diameter 3 µm) with a precolumn (Mesopore 50 × 7.5 mm) operating at 30 °C. THF at a flow rate of 0.30 mL min-1 was used as eluent. The mass spectrometer was coupled to the column in parallel to an UV-detector (VWD 3400, Dionex), and a RI-detector (RefractoMax520, ERC, Japan). 0.27 mL min-1 of the eluent were directed through the UV- and RI-detector and 30 µL min-1 were infused into the electrospray source after post-column addition of a 50 µM solution of sodium iodide in methanol at 20 µL min-1 by a micro-flow HPLC syringe pump (Teledyne ISCO, Model 100DM). A 200 µL aliquot of a polymer solution with a concentration of 2 mg mL-1 was injected into the SEC system. SEC-ESI-MS simulation was performed with a published software package.[5]

Stationary UV-Vis Absorption Spectroscopy

UV-Vis spectra were recorded on a Shimadzu UV-2700 spectrophotometer equipped with a CPS-100 electronic temperature control cell positioner. Stock solutions of samples were prepared in H_2O with a concentration of 10 mg mL^{-1} and measured in Hellma Analytics quartz cuvettes at 25 °C.

Rheological Experiments

Rheological experiments were carried out using an Anton Paar rheometer with a plate-plate configuration. The lower plate is made of quartz and the upper plate of stainless steel with a diameter of 25 mm. The LED light source (445 nm or 525 nm, intensity was tuned to 20 mW cm^{-2}) was placed underneath the quartz plate. In a typical experiment, 50 µL of an aqueous solution of polymers (10 wt%, ca. 4.7 mM), was placed on the lower plate and the upper plate was brought to a measurement gap of 0.3 mm. The test was started by applying a 0.1% strain with the frequency of 1 Hz on the sample, and the light was turned on at predetermined interval. Light sources were commercially available LEDs with a 10 W power output.

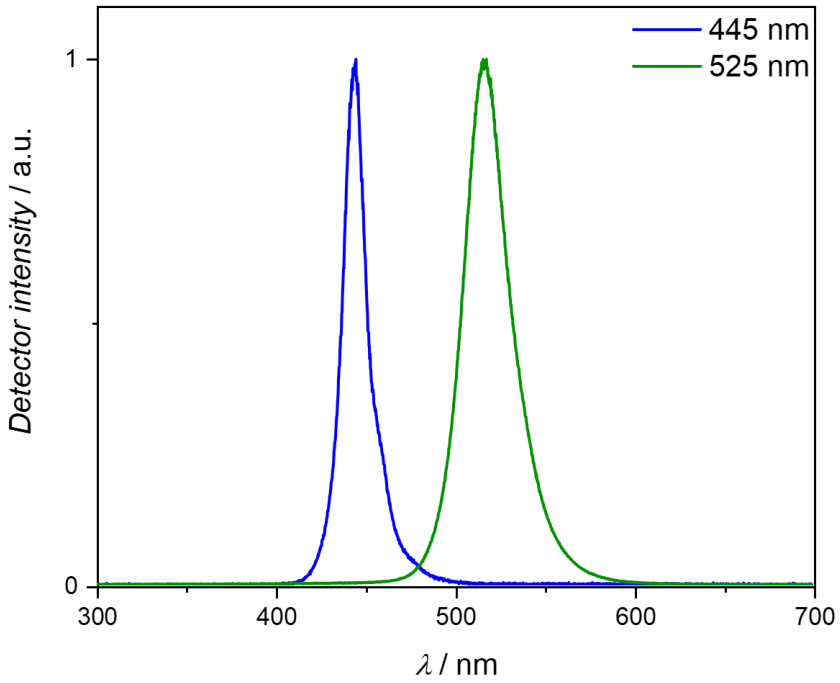

Figure S1. Emission spectra of the LED lights used in the irradiation experiments.

Wavelength Resolved Pulsed Laser Experiments

Laser irradiation experiments were conducted using the apparatus shown in **Figure S2**. The procedure has been established in our laboratories and the below description is the standard text used in all our publications describing the process. The light source was an Opotek Opolette 355 OPO, producing 7 ns, 20 Hz pulses with a flattop spatial profile. The output beam was initially passed through a beam expander (-50 mm and 100 mm lens combination) to ensure it is large enough to uniformly irradiate the entire sample volume. The beam then passes through an electronic shutter and directed upwards using a UV silica right angle prism. Finally, the beam enters the sample, suspended in an aluminum block, from below. The laser energy deposited into the sample was measured above the aluminum block before and after experiments using a Coherent EnergyMax thermopile sensor (J-25MB-LE) to account for any power fluctuations during irradiation.

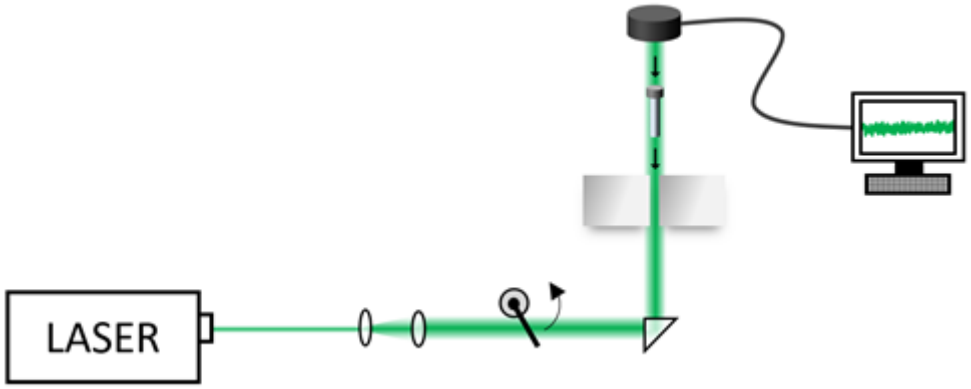

Figure S2. Apparatus used for the laser experiments (action plots).

Precise photon numbers were determined from the laser pulse energy using the following relation

$$N_p = \frac{E_{pulse} \cdot \lambda \cdot f_{rep} \cdot t}{hc \cdot \frac{T_\lambda}{100}} \quad (1)$$

where E_{pulse} is the measured pulse energy above the aluminum block, λ is the wavelength of the incident radiation, f_{rep} is the laser repetition rate, t is the irradiation time, h is Planck's constant, c is the speed of light and T_λ is the wavelength dependent glass transmission presented in **Figure S3**. For laser measurements, all samples were prepared in 0.7 mL glass crimp vials (ID 6.2 mm) capped with a rubber/PTFE septum. Once an initial measurement is completed and the photon number is known, the required energies at other wavelengths can be found by rearranging equation 1 to give

$$E_{pulse} = \frac{N_P \cdot hc \cdot \frac{T_\lambda}{100}}{\lambda \cdot f_{rep} \cdot t} \quad (2)$$

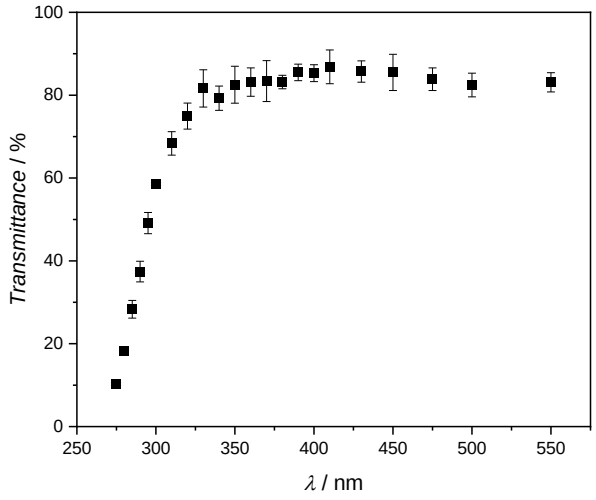

Figure S3. Transmittance of the bottom of the glass vials used in the current study. The transmittance values shown and used here were obtained analogously to a method reported previously.[1] The glass vials were cut at a height of 3 mm.

The transmittance values shown and used here were obtained analogously to a method reported previously.[1] The glass vials were cut at a height of 3 mm.

General Procedure for Pulsed Laser Irradiation of SPP-PEG and AP-PEG in Aqueous Solutions[2, 6]

Stock solutions of 10 mg mL-1 of MeO-PEG-SPP or MeO-PEG-AP in aqueous media were prepared. The aqueous solutions were prepared prior to use and stored at ambient temperature. 100 µL was injected into a glass vial, suitable for pulsed laser irradiation (refer to the section *'Wavelength Resolved Pulsed Laser Experiments'* for details). All samples were degassed with a constant stream of nitrogen for 10 min prior to irradiation. The output energy of the nanosecond laser was adjusted to ensure constant photon numbers deposited across all samples. All samples were irradiated for 1800 seconds if not stated otherwise. After irradiation, the irradiated volume (100 µL) was split into aliquots of 25 uL volume. One aliquot was dissolved in 1775 µL THF, filtered and submitted to SEC, the other aliquot was diluted in 2475 µL of the respective solvent used for irradiation prior to submission to stationary UV-Vis spectroscopy.

General Procedure for the Calculation of Conversion from SEC Data

UV traces (254 nm absorption) of each sample are used for calculation. UV absorption versus the retention volume was plotted for the entire sample set. The trace, consisting of MeO-PEG-SPP and (MeO-PEG-SPP)2 (or MeO-PEG-AP and dimer) was deconvoluted with two Gaussian functions, representing the two species. The Conversion, X, was then calculated via equation 3:

$$X = \frac{Area_{Dimer}}{Area_{Dimer} + Area_{Monomer}} \quad (3)$$

With $Area_{Dimer}$ being the area under the dimer species obtained by SEC after irradiation and $Area_{Monomer}$ being the area under the monomer species after irradiation.

The error in conversion X, ΔX, was estimated according to a simple error propagation method:

$$\Delta X = \sqrt{\left[\frac{\partial X}{\partial Area_{Dimer}}\right]^2 \cdot \Delta Area_{Dimer}{}^2 + \left[\frac{\partial X}{\partial Area_{Monomer}}\right]^2 \cdot \Delta Area_{Monomer}{}^2} \quad (4)$$

$$\Delta X = \sqrt{\left[\frac{Area_{Monomer}}{(Area_{Dimer} + Area_{Monomer})^2}\right]^2 \cdot [0.1 Area_{Dimer}]^2 + \left[\frac{-Area_{Dimer}}{(Area_{Monomer} + Area_{Dimer})^2}\right]^2 \cdot [0.1 Area_{Monomer}]^2} \quad (5)$$

The error in the respective areas of monomer and dimer species was assumed to be 10% of the original area value. The errors are displayed in form of error bars.

1.3. Synthetic Procedures

*3-Methylpyrido[2,3-b]pyrazine (**S1**)*

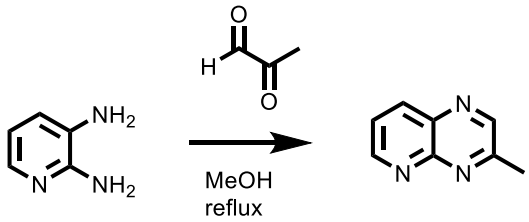

S1

Methylglyoxal (40% in water, 5.4 g, 0.03 mmol) was added to a solution of pyridine-2,3-diamine (2.18 g, 0.02 mol) in methanol (40 mL) and the solution was heated at 80 °C with stirring under refluxing conditions for 3 h. The solution was subsequently concentrated in vacuo and the crude product was purified by column chromatography eluting with hexane: ethylacetate (v/v = 1/9) to give product as dark solid (yield: 2.73 g, 94%). ^{1}H NMR ($CDCl_3$, 400 MHz) δ 9.15 (dd, 1H, J=4.2 and 1.9 Hz), 8.85 (s, 1H), 8.45 (dd, 1H, J=8.3 and 1.9 Hz), 7.68 (dd, 1H, J=8.3 and 4.2Hz), 2.88 (s, 3H). ^{1}H NMR is in agreement with previously published literature.[7]

*Ethyl (E)-4-(2-methoxy-4-(2-(pyrido[2,3-b]pyrazin-3-yl)vinyl)phenoxy)butanoate (**S2**)*

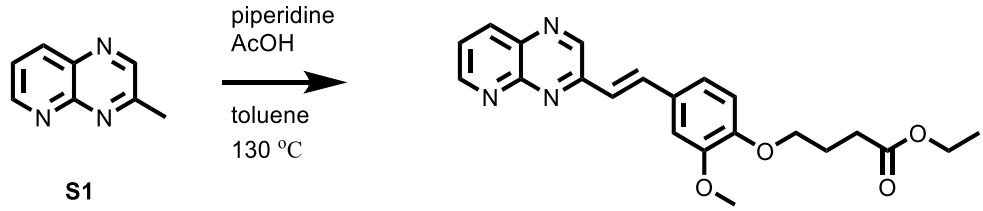

S1

S2

To a mixture of **S1** (1.44, 0.01 mol) and ethyl 4-(4-formyl-2-methoxyphenoxy)butanoate[2] (4 g, 0.015 mol), piperidine (0.425 g, 5 mmol), acetic acid (0.42 g, 7 mmol) and dry toluene (5 mL) were added. The mixture was purged with Argon, sealed and heated at 120 °C for 48 h. The resultant solution was concentrated in vacuo and absorbed onto silica gel. The product was purified by column chromatography running with hexane: ethyl acetate (v/v = 5/5) to give pure product as orange solid (yield: 2.1 g, 53.9%).^{1}H NMR ($CDCl_3$, 600 MHz): δ 9.14 (dd, 1H, J=4.1 and 2.0 Hz), 9.03 (s, 1H), 8.42 (dd, 1H, J=8.2 and 2 Hz), 8.1 (d, 1H, J=8.4 H) , 7.62-7.65 (dd, 1H, J=8.2 and 4.2 Hz), 7.22-7.3 (m, 3H), 6.92-6.94 (d, 1H, J=4.1 Hz), 4.13-4.16 (m, 4H), 3.91 (s, 3H), 2.53-2.57 (t, 2H, J=7.2 Hz), 2.17-2.21 (m, 2H), 1.25-1.28 (t, 3H, J=7.2 Hz).

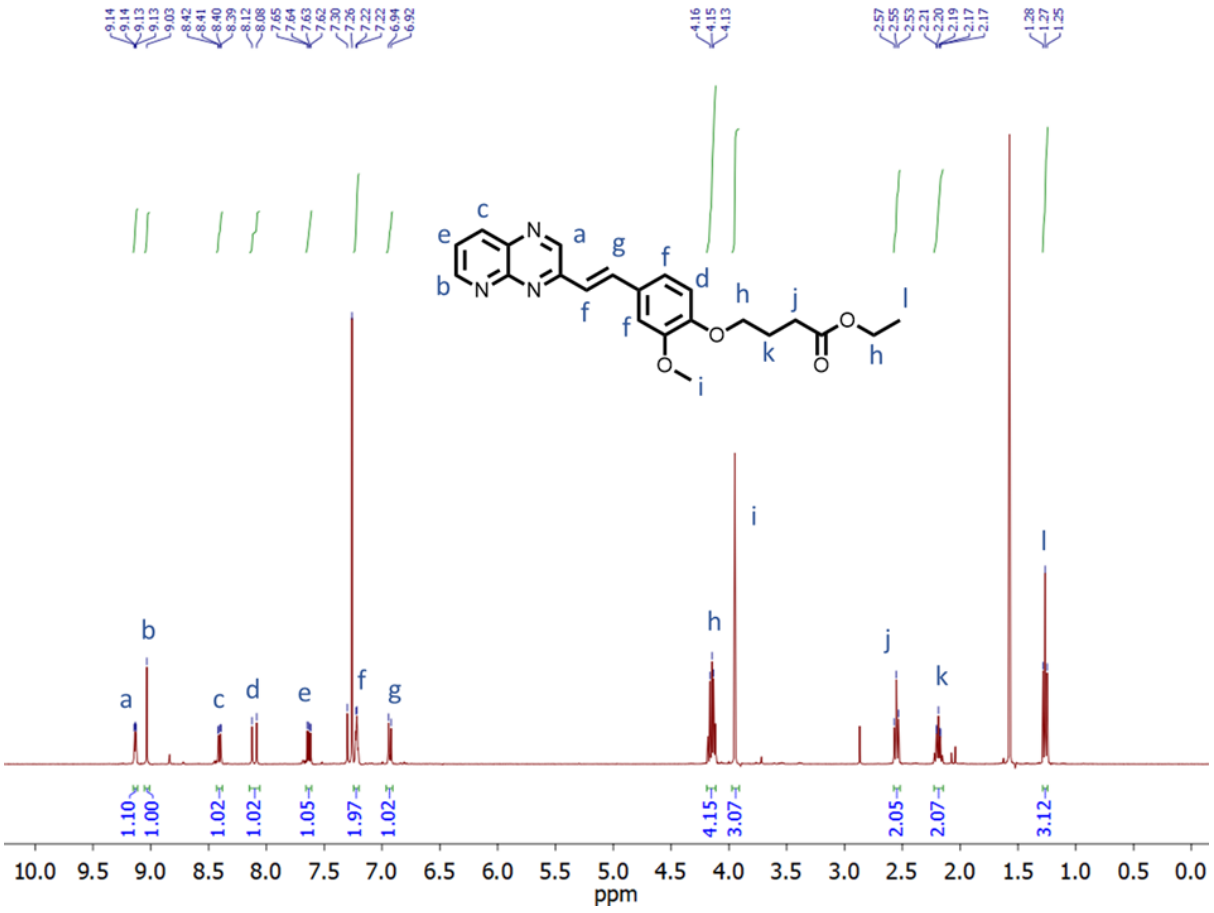

Figure S4. ^{1}H NMR spectrum of **S2** ($CDCl_3$, 600 MHz).

*(E)-4-(2-methoxy-4-(2-(pyrido[2,3-b]pyrazin-3-yl)vinyl)phenoxy)butanoic acid (**S3**).*

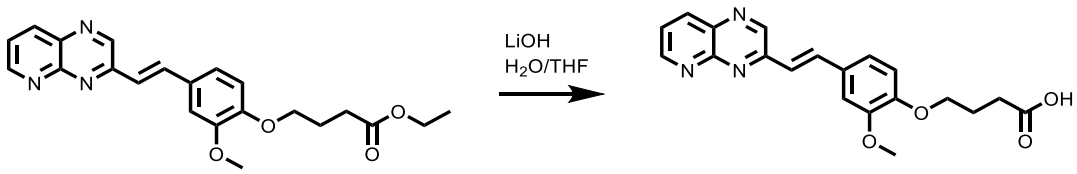

S2 **S3**

Compound **S2** (1.85 g, 5 mmol) was dissolved in THF (10 mL) and to this solution was added a solution of LiOH (0.5 g, 20 mmol) in deionised water (10 mL). The solution was stirred at ambient temperature for 1 h and carefully neutralised with acetic acid. Addition of excess acetic acid resulted in the precipitation of an orange product which was filtered, washed with copious amount of water, dried in vacuo and used directly in the next step (yield: 1.21 g, 66.3%).

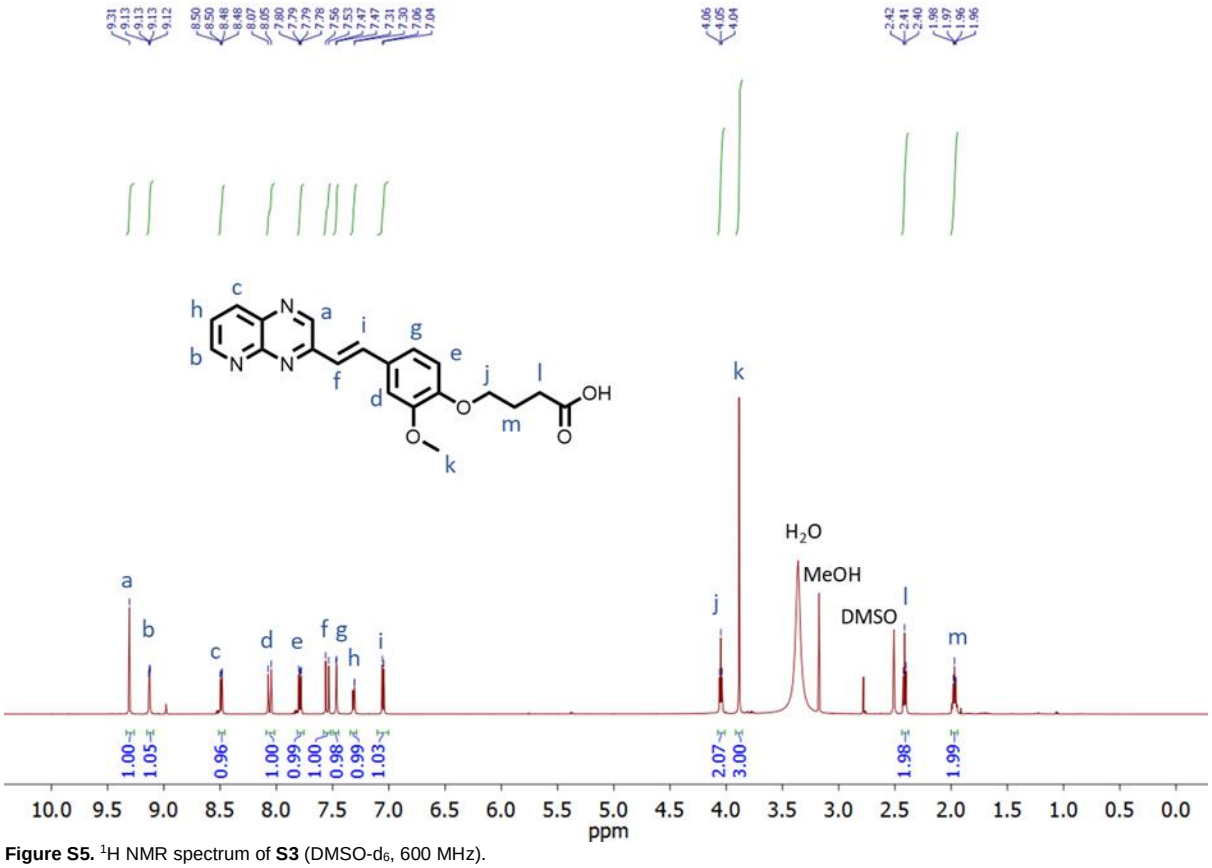

Figure S5. ^{1}H NMR spectrum of **S3** (DMSO-d_6, 600 MHz).

*2,5-Dioxopyrrolidin-1-yl(E)-4-(2-methoxy-4-(2-(pyrido[2,3-b]pyrazin-3-yl)vinyl)phenoxy)butanoate (**S4**)*

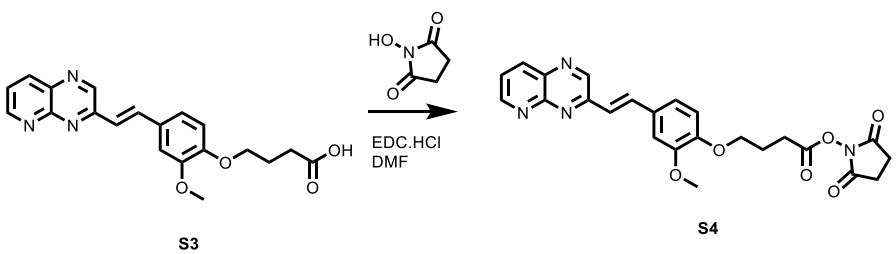

S3 **S4**

Compound **S3** (1.2 g, 3.3 mmol) was dissolved in DMF (10 mL) and to the solution was added EDC.HCl (0.8 g, 4.1 mmol) and N-hydroxysuccinimide (0.46 g, 4.1 mmol). The solution was stirred at ambient temperature for 3 h and DMF was concentrated in vacuo. The crude product was absorbed onto silica gel and purified by column chromatography eluting with hexane/ethylacetate (v/v = 7/3) to give product as orange crystal (yield: 1.04 g, 68%). ^{1}H NMR (CD_2Cl_2, 600 MHz): δ 9.14 (dd, 1H, J=4.1 and 2.0 Hz), 9.03 (s, 1H), 8.42 (dd, 1H, J=8.2 and 2 Hz), 8.1 (d, 1H, J=8.4 H) , 7.62-7.65 (dd, 1H, J=8.2 and 4.2 Hz), 7.22-7.3 (m, 3H), 6.92-6.94 (d, 1H, J=4.1 Hz), 4.18-4.2 (t, J=7.2 Hz, 2H), 3.98 (s, 3H), 2.94-2.91 (t, 2H, J=7.2 Hz), 2.86 (s, 4H), 2.28-2.31 (m, 2H). ^{13}C NMR (CD_2Cl_2, 151 MHz) δ 169.74, 169.07, 154.83, 154.40, 151.76, 150.54, 150.51, 146.52, 138.75, 138.50, 137.39, 129.91, 124.67, 123.10, 122.48, 113.94, 110.69, 67.78, 56.48, 28.21, 26.21, 25.06. LC-MS (ESI) m/zexp: 463.1606, m/ztheo: 463.1612 ([M+H]+), Δ / ppm: 1.30.

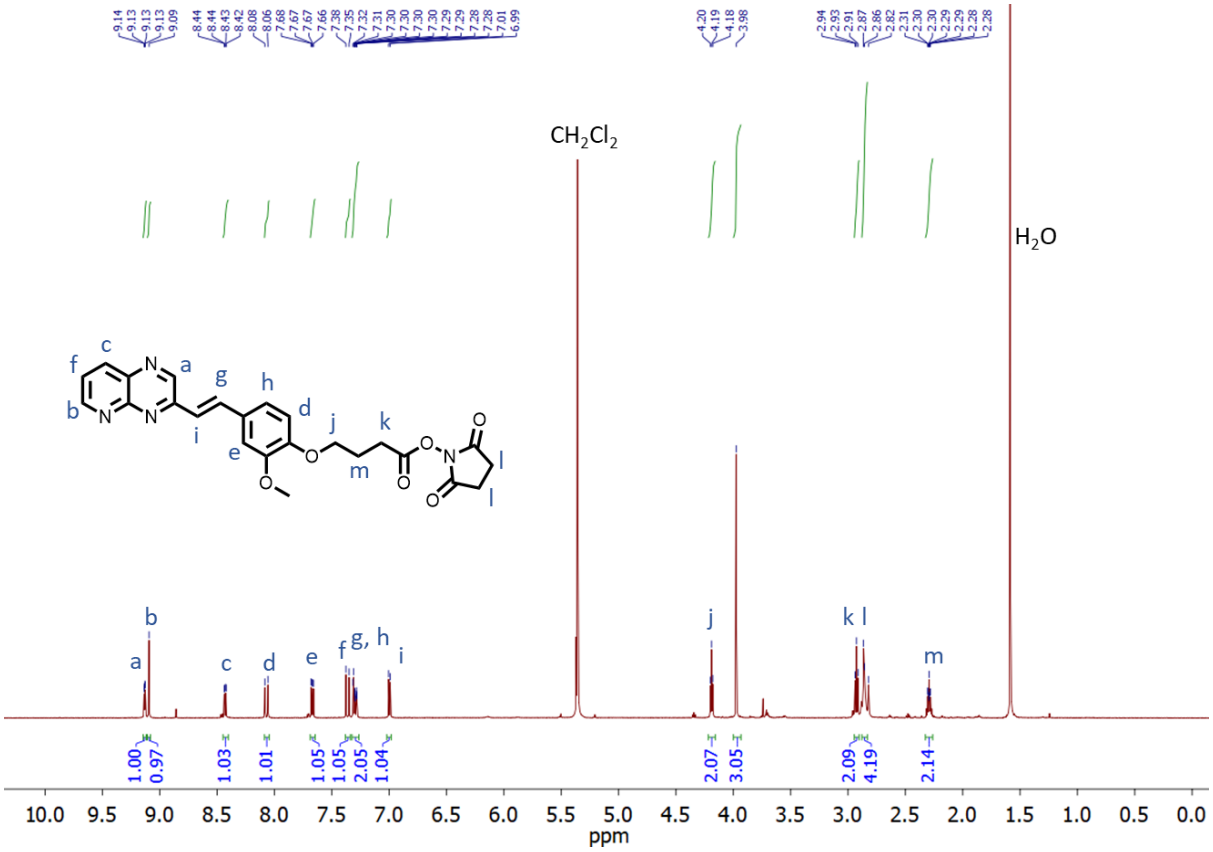

Figure S6. ^{1}H NMR spectrum of **S3** (DMSO-d_6, 600 MHz).

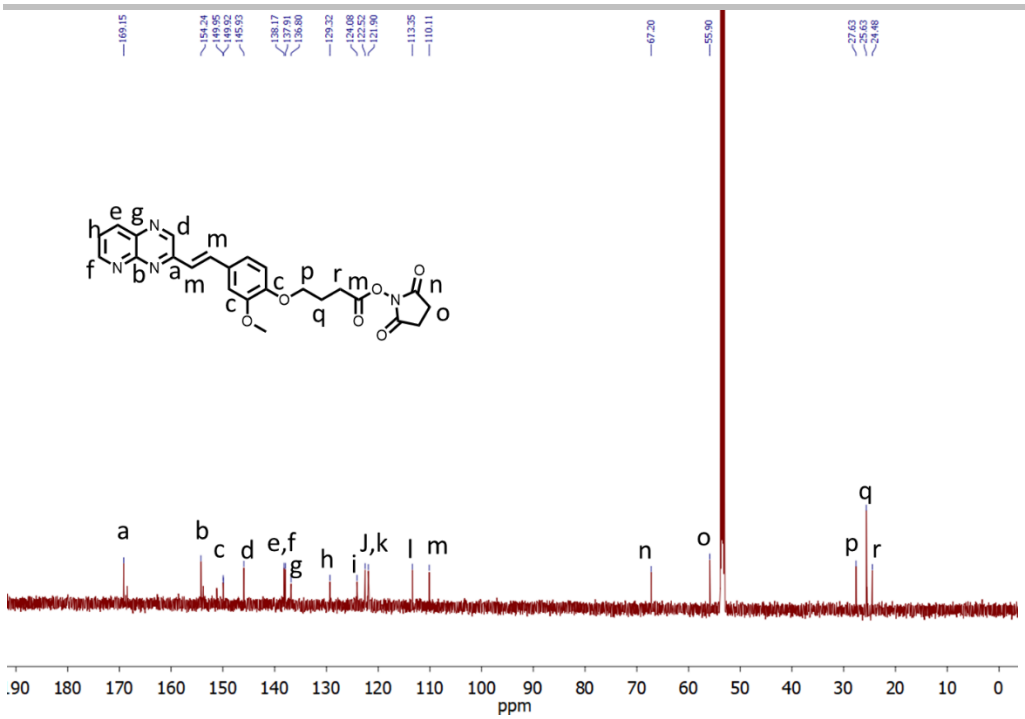

Figure S7. ^{13}C NMR spectrum of **S3** (DMSO-d_6, 151 MHz).

MeO-PEG-SPP

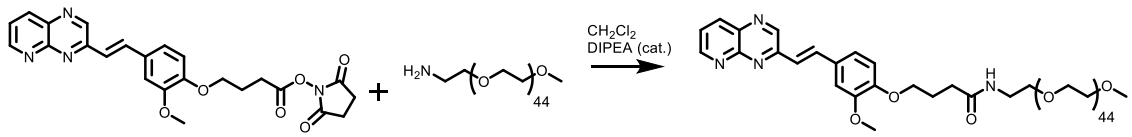

MeO-PEG-NH_2 (0.5 g, 0.25 mmol) was dissolved in CH_2Cl_2 (5 mL) and compound **S4** (108 mg, 0.26 mmol) was added followed by addition of DIPEA (10 µL). The solution was stirred at ambient temperature for 3 h and precipitated into diethyl ether (100 mL) to afford the product as a yellow solid (yield: 0.52 g, 86%).

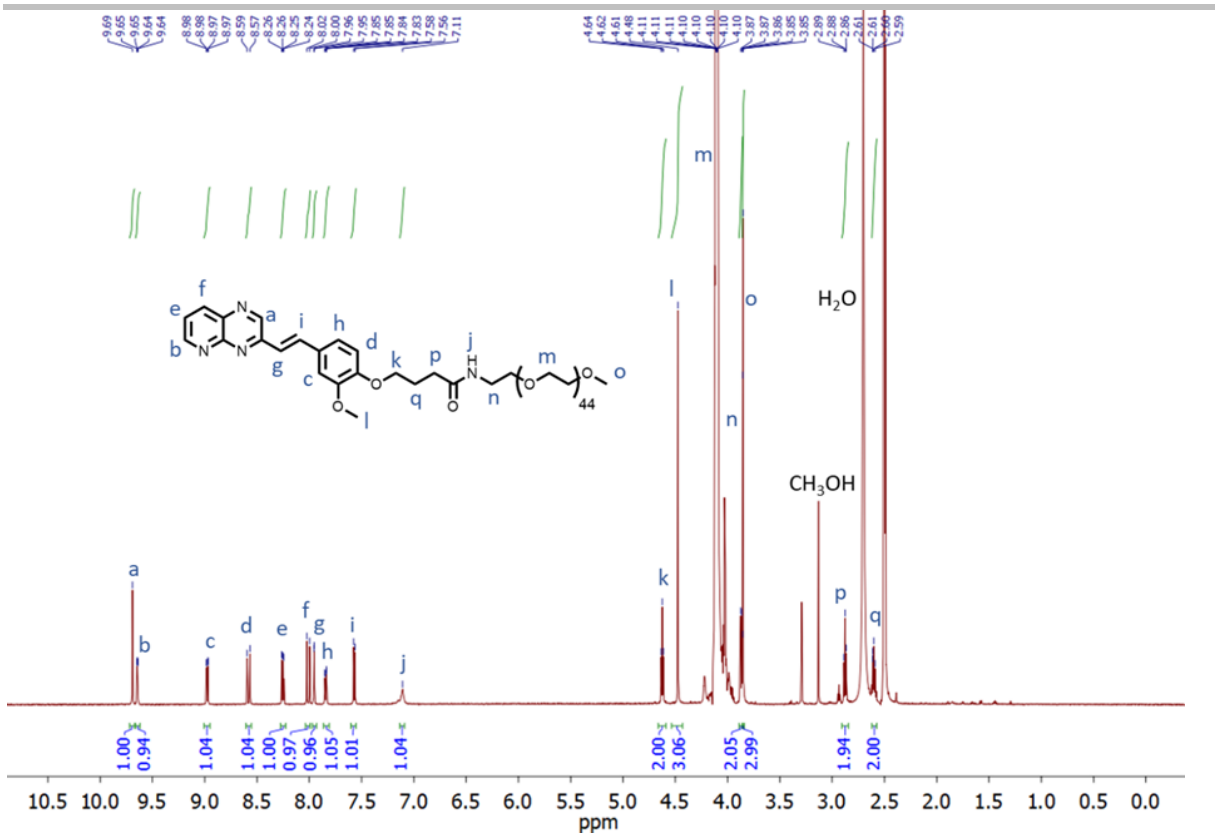

Figure **S8**. ^{1}H NMR spectrum of **MeO-PEG-SPP** (d_6-DMSO, 600 MHz).

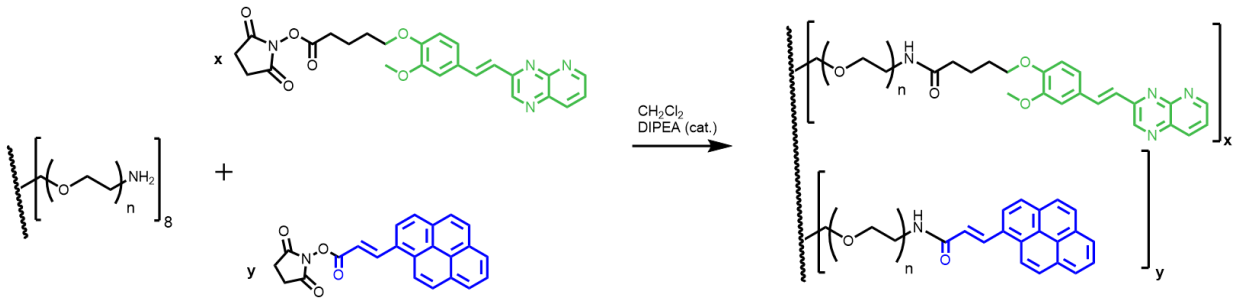

Scheme S1. Synthesis of 8-arm PEG containing SPP or AP, or both SPP and AP endgroups.

PEG-(SPP)$_8$

PEG-(SPP)$_8$ was synthesized from PEG-(NH$_2$)$_8$ and compound S4 using a similar procedure to the synthesis of MeO-PEG-SPP, affording the product as a yellow solid with a yield of 94%.

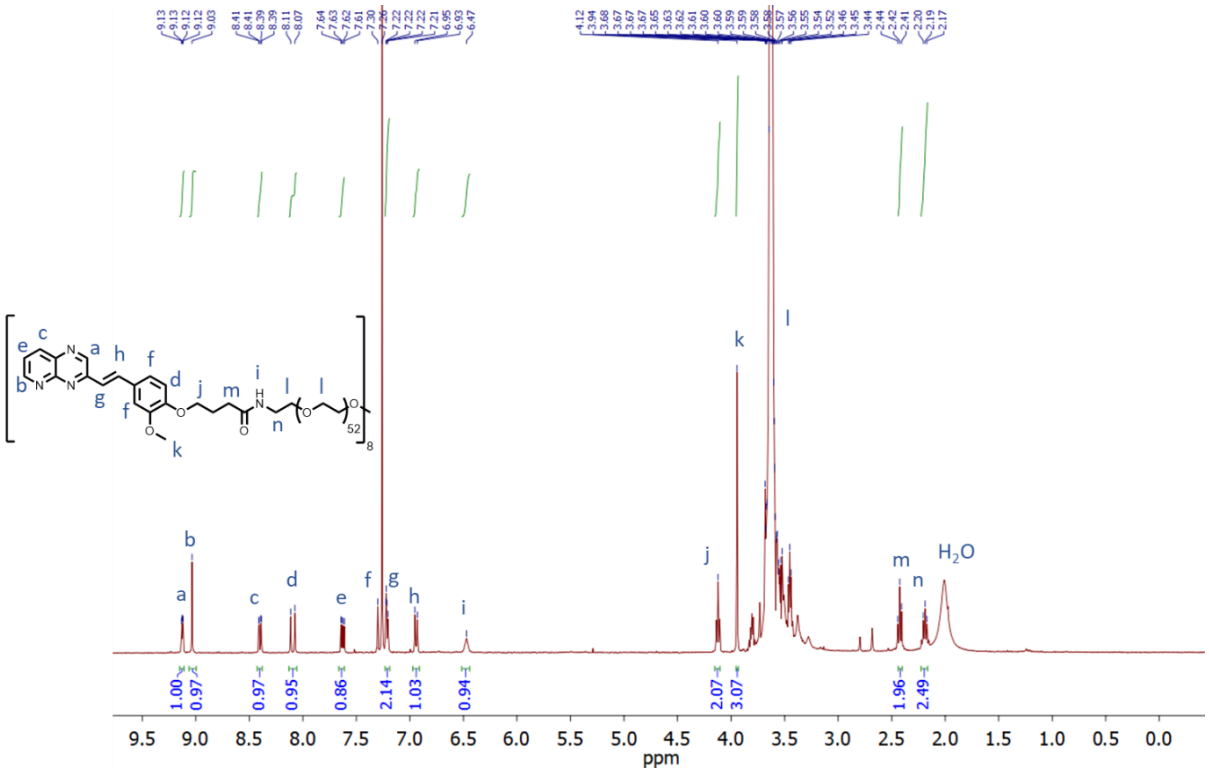

Figure S9. ^{1}H NMR spectrum of **PEG-(SPP)$_8$** ($CDCl_3$, 400 MHz).

PEG-(AP)$_8$

PEG-(AP)$_8$ was synthesized from PEG-$(NH_2)_8$ and 3-(pyren-1-yl)acrylate-N-hydroxysuccinimide[3] using a similar procedure to the synthesis of MeO-PEG-SPP, affording the project as a yellow solid with a yield of 97%.

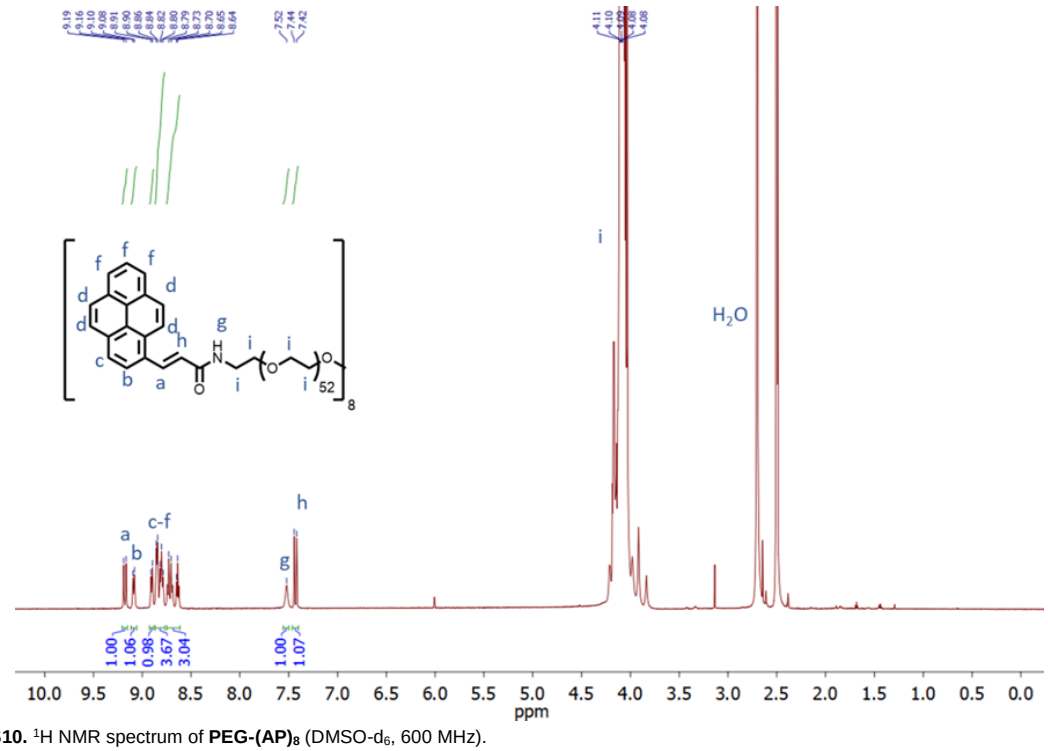

Figure S10. ^{1}H NMR spectrum of **PEG-(AP)$_8$** (DMSO-d_6, 600 MHz).

SUPPORTING INFORMATION

*(E)-3-(2-(2-hydroxystyryl)-3,3-dimethyl-3H-indol-1-ium-1-yl)propane-1-sulfonate (**PAG**)*

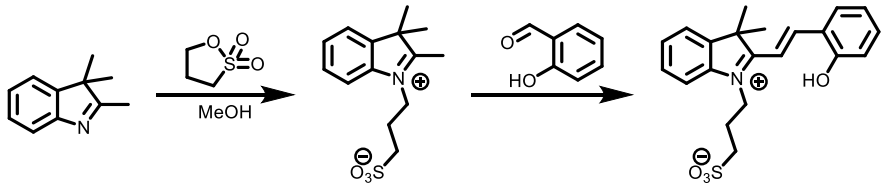

PAG

2,3,3-trimethylindolenine (1.65 g, 0.01 mmol) was added into propane sultone (1.26 g, 0.01) and the mixture was stirred at 90 °C for 4 h. Upon cooling to room temperature, methanol (5 mL) was added and stirred for 10 min, followed by addition of diethyl ether (50 mL). The solid was filtered and washed with diethyl ether and dried in vacuo to give product as purple solid (yield: 2.1 g, 75%).

The above solid (1 g, 3.6 mmol) was dissolved in ethanol (20 mL) and 2-hydroxybenzaldehyde (0.48 g, 3.9 mmol). The mixture was heated at 90 °C under refluxing condition for 14 h. Upon cooling to room temperature the mixture was filtered and the solid was washed with ice-cold ethanol, dried in vacuo to give product as yellow solid (yield: 1 g, 73%). ^{1}H NMR (600 MHz, d_6-DMSO): δ = 11.03 (s, 1H), 8.62 (d, 1H, J = 16.5), 8.28 (d, 1H, J = 7.0), 8.02 (d, 1H, J = 7.0), 7.87 (m, 2H), 7.62 (m, 2H), 7.45 (t, 1H, J = 8.4), 7.04 (d, 1H, J = 8.5), 6.96 (t, 1H, J = 7.0), 4.80 (t, 2H, J = 7.5), 2.65 (t, 2H, J = 6.0), 2.15 (m, 2H), 1.78 (s, 6H).). ^{13}C NMR (d_6-DMSO, 151 MHz) δ = 181.77, 159.02, 148.70, 143.48, 140.93, 135.75, 129.77, 129.15, 129.13, 122.98, 121.34, 120.07, 116.62, 115.09, 111.45, 51.90, 47.33, 45.54, 26.44, 24.58. LC-MS (ESI): *m/z* $[M+H]^+$, sim: 386.1421, exp: 386.1419, *Δ* / ppm: 0.52.

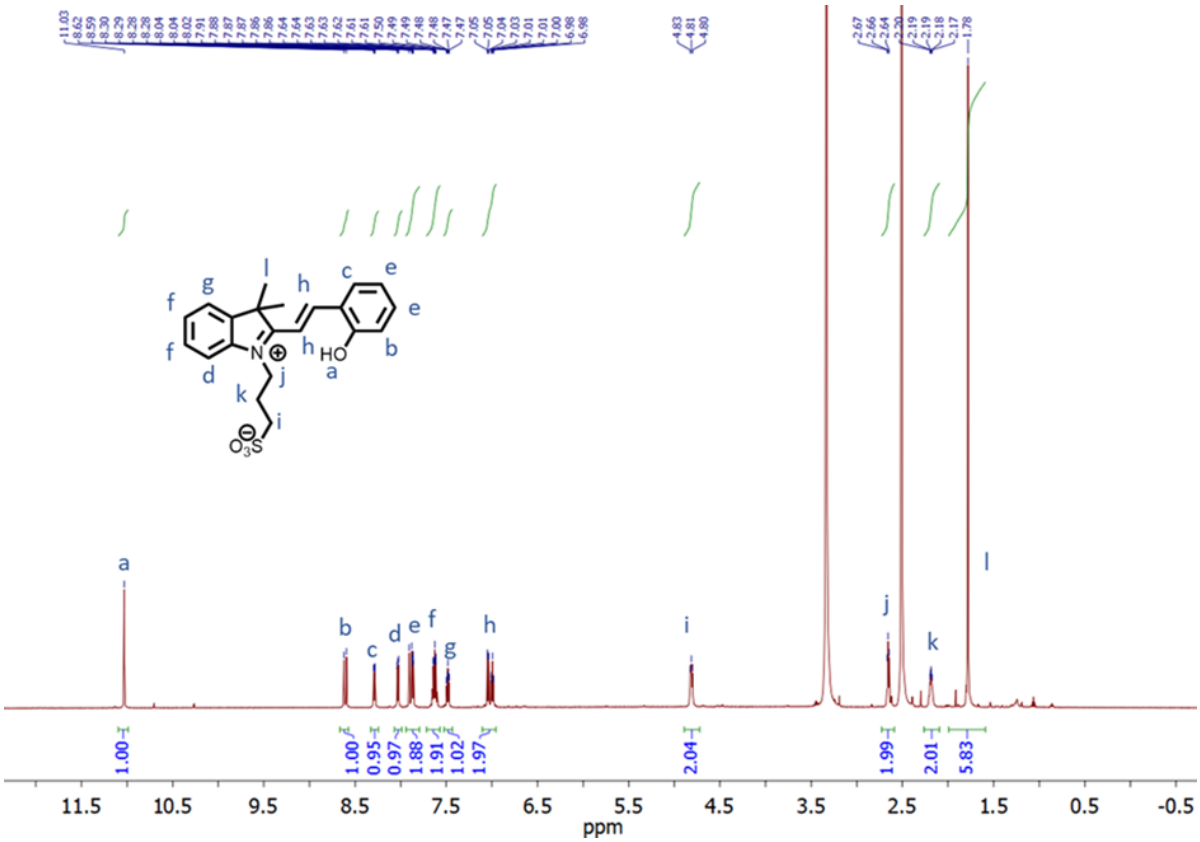

Figure S6. ^{1}H NMR spectrum of **PAG** (d_6-DMSO, 600 MHz).

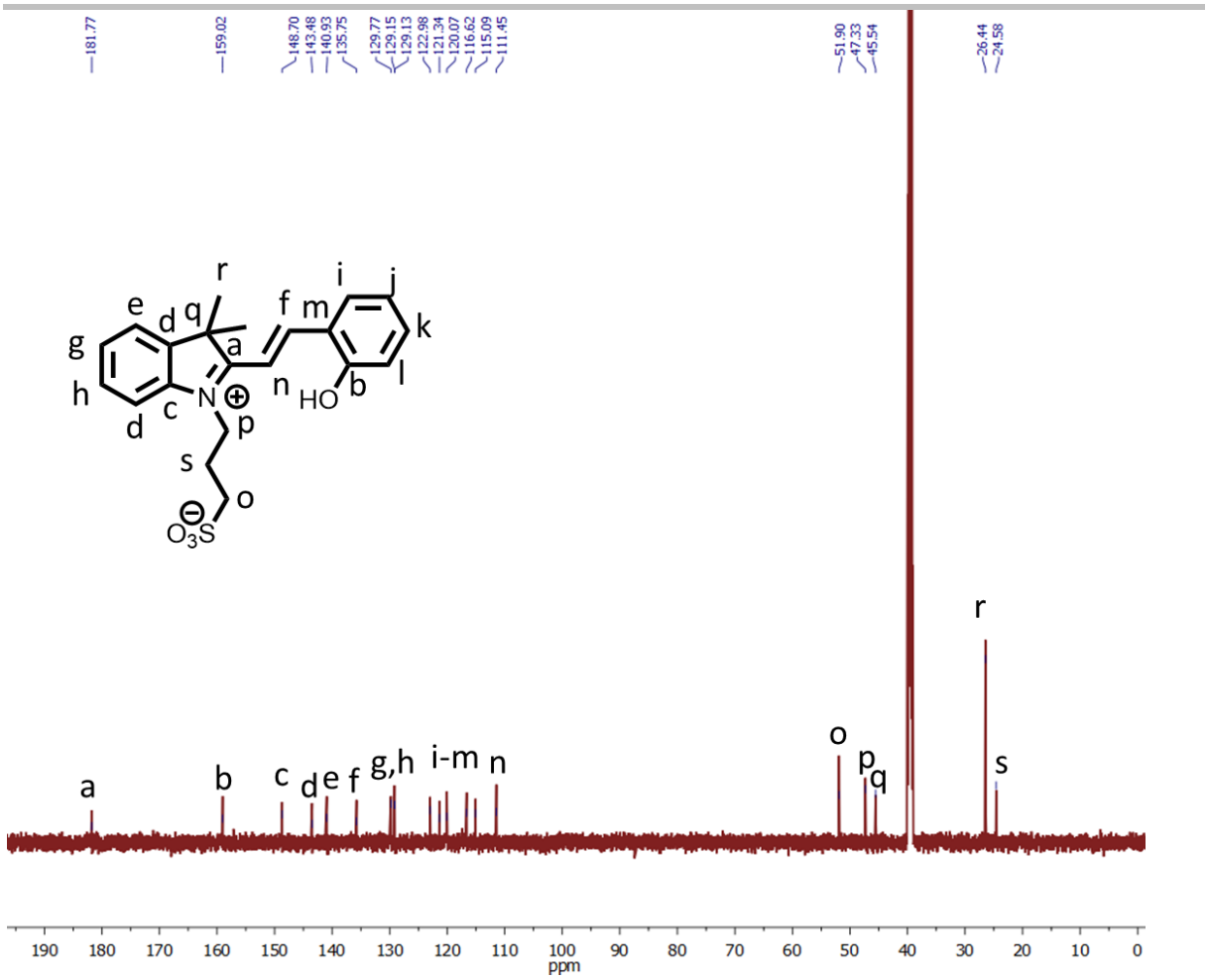

Figure S12. ^{13}H NMR spectrum of **PAG** (d_6-DMSO, 153 MHz).

Additional Experimental Data

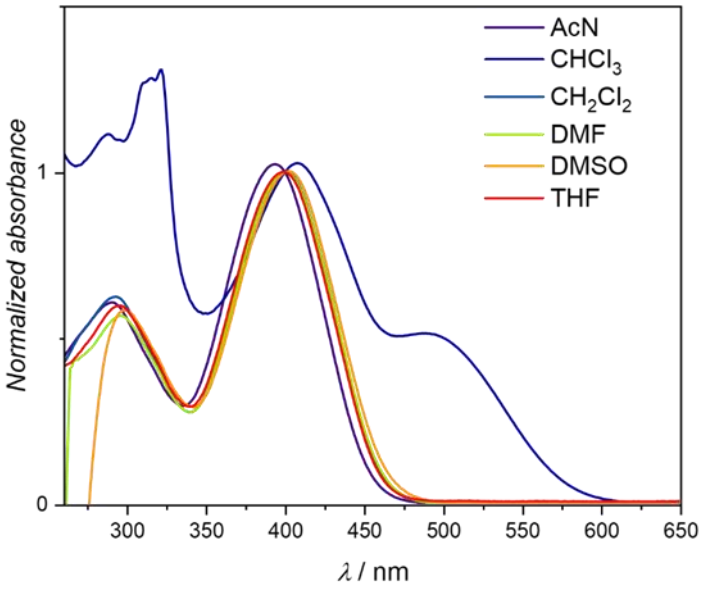

Figure S13. Stationary UV/Vis spectra of **MeO-PEG-SPP** in different organic solvents. Spectra were normalised to the absorbance at 400 nm.

Table S1. Experimental data for the irradiation of **MeO-PEG-SPP** in aqueous solution. λ: Wavelength, E_{pulse}: Measured pulse energy at the sample holder of the laser setup (**Figure S2**), ΔE_{pulse}: Error in measured pulse energy, t: Irradiation time, T_λ: Transmittance of the glass vial at respective wavelength, N_P: Deposited number of photons according to eq. 1, ΔN_P: Error in deposited number of photons, X: Conversion according to eq. 3, ΔX: Error in conversion according to eq. 5.

λ / nm	E_{pulse} / µJ	ΔE_{pulse} / µJ	t / s	T_λ	N_P / µmol	ΔN_P / µmol	X	ΔX
-	0	0	0		0	0	0	0.00
410	882	84	2040	85.13	104.92	9.99	0.40	0.03
420	986	54	1800	85.24	106.15	5.81	0.29	0.03
440	929	25	1800	85.36	104.93	2.82	0.32	0.03
460	890	16	1800	85.41	105.16	1.89	0.39	0.03
480	848	22	1800	85.43	104.58	2.71	0.51	0.04
500	816	20	1800	85.44	104.84	2.57	0.35	0.03
520	789	24	1800	85.45	105.43	3.21	0.17	0.02
540	755	32	1800	85.45	104.77	4.44	0.04	0.00
560	728	31	1800	85.45	104.77	4.46	0.00	0.00
580	700	44	1800	85.45	104.33	6.56	0.00	0.00
600	680	40	1800	85.45	104.85	6.17	0.00	0.00

Table S2. Experimental data for the irradiation of **MeO-PEG-SPP** in aqueous solution (pH=5). λ: Wavelength, E_{pulse}: Measured pulse energy at the sample holder of the laser setup (**Figure S2**), $\Delta E_{pulse:}$ Error in measured pulse energy, t: Irradiation time, T_λ: Transmittance of the glass vial at respective wavelength, N_P: Deposited number of photons according to eq. 1, ΔN_P: Error in deposited number of photons, X: Conversion according to eq. 3, ΔX: Error in conversion according to eq. 5.

λ / nm	E_{pulse} / µJ	ΔE_{pulse} / µJ	t / s	T_λ	N_P / µmol	ΔN_P / µmol	X	ΔX
	0	0	0		0	0	0	0.00
410	768	48	2340	85.13	104.80	6.55	0.15	0.02
420	981	56	1800	85.24	105.62	6.03	0.13	0.02
440	926	28	1800	85.36	104.59	3.16	0.17	0.02
460	886	17	1800	85.41	104.68	2.01	0.14	0.02
480	847	21	1800	85.43	104.46	2.59	0.16	0.02
500	813	19	1800	85.44	104.45	2.44	0.15	0.02
520	781	24	1800	85.45	104.36	3.21	0.06	0.01
540	758	30	1800	85.45	105.19	4.16	0.01	0.00
560	724	32	1800	85.45	104.19	4.61	0.01	0.00
580	704	40	1800	85.45	104.93	5.96	0.01	0.00
600	681	40	1800	85.45	105.00	6.17	0.01	0.00

Table S3. Experimental data for the irradiation of **MeO-PEG-SPP** in aqueous solution (pH=3). λ: Wavelength, E_{pulse}: Measured pulse energy at the sample holder of the laser setup (**Figure S2**), $\Delta E_{pulse:}$ Error in measured pulse energy, t: Irradiation time, T_λ: Transmittance of the glass vial at respective wavelength, N_P: Deposited number of photons according to eq. 1, ΔN_P: Error in deposited number of photons, X: Conversion according to eq. 3, ΔX: Error in conversion according to eq. 5.

λ / nm	E_{pulse} / µJ	ΔE_{pulse} / µJ	t / s	T_λ	N_P / µmol	ΔN_P / µmol	X	ΔX
-	0	0	0		0	0	0.01	0.00
410	760	81	2360	85.13	104.59	11.15	0.18	0.02
420	972	60	1800	85.24	104.65	6.46	0.15	0.02
440	928	31	1800	85.36	104.81	3.50	0.18	0.02
460	891	18	1800	85.41	105.27	2.13	0.17	0.02
480	850	23	1800	85.43	104.83	2.84	0.19	0.02
500	814	23	1800	85.44	104.58	2.95	0.17	0.02
520	790	23	1800	85.45	105.56	3.07	0.08	0.01
540	761	35	1800	85.45	105.60	4.86	0.03	0.00
560	725	33	1800	85.45	104.33	4.75	0.01	0.00
580	702	43	1800	85.45	104.63	6.41	0.01	0.00
600	682	46	1800	85.45	105.16	7.09	0.01	0.00

Table S4. Experimental data for the irradiation of **MeO-PEG-SPP** in aqueous solution (pH=1). λ: Wavelength, E_{pulse}: Measured pulse energy at the sample holder of the laser setup (**Figure S2**), $\Delta E_{pulse:}$ Error in measured pulse energy, t: Irradiation time, T_λ: Transmittance of the glass vial at respective wavelength, N_P: Deposited number of photons according to eq. 1, ΔN_P: Error in deposited number of photons, X: Conversion according to eq. 3, ΔX: Error in conversion according to eq. 5.

λ / nm	E_{pulse} / µJ	ΔE_{pulse} / µJ	t / s	T_λ	N_P / µmol	ΔN_P / µmol	X	ΔX
-	0	0	0		0	0	0.01	0.00
410	709	80	2540	85.13	105.01	11.85	0.03	0.00
420	976	67	1800	85.24	105.08	7.21	0.02	0.00
440	923	32	1800	85.36	104.25	3.61	0.01	0.00
460	885	18	1800	85.41	104.57	2.13	0.01	0.00
480	853	23	1800	85.43	105.20	2.84	0.01	0.00
500	821	23	1800	85.44	105.48	2.95	0.01	0.00
520	787	30	1800	85.45	105.16	4.01	0.01	0.00
540	756	41	1800	85.45	104.91	5.69	0.00	0.00
560	731	37	1800	85.45	105.20	5.32	0.00	0.00
580	702	46	1800	85.45	104.63	6.86	0.00	0.00
600	677	49	1800	85.45	104.38	7.56	0.01	0.00

Table S5. Experimental data for the irradiation of **MeO-PEG-SPP** in H_2O in the presence of PAG in [PAG]=1.71 mg mL^{-1} (stochiometric amount). λ: Wavelength, E_{pulse}: Measured pulse energy at the sample holder of the laser setup (**Figure S2**), $\Delta E_{pulse:}$ Error in measured pulse energy, t: Irradiation time, T_λ: Transmittance of the glass vial at respective wavelength, N_P: Deposited number of photons according to eq. 1, ΔN_P: Error in deposited number of photons, X: Conversion according to eq. 3, ΔX: Error in conversion according to eq. 5.

λ / nm	E_{pulse} / µJ	ΔE_{pulse} / µJ	t / s	T_λ	N_P / µmol	ΔN_P / µmol	X
-	0	0	0		0	0	0.01
410	1010	91	1800	85.13	106.01	9.55	0.17
420	969	56	1800	85.24	104.32	6.03	0.17
440	930	28	1800	85.36	105.04	3.16	0.21
460	886	20	1800	85.41	104.68	2.36	0.15
480	851	27	1800	85.43	104.95	3.33	0.19
500	818	25	1800	85.44	105.10	3.21	0.18
520	780	28	1800	85.45	104.23	3.74	0.08
540	756	41	1800	85.45	104.91	5.69	0.03
560	728	41	1800	85.45	104.77	5.90	0.01
580	707	52	1800	85.45	105.38	7.75	0.01
600	682	49	1800	85.45	105.16	7.56	0.01

Table S6. Experimental data for the irradiation of **MeO-PEG-SPP** in H_2O in the presence of PAG in [PAG]=4.00 mg mL^{-1} . λ: Wavelength, E_{pulse}: Measured pulse energy at the sample holder of the laser setup (**Figure S2**), $\Delta E_{pulse:}$ Error in measured pulse energy, t: Irradiation time, T_λ: Transmittance of the glass vial at respective wavelength, N_P: Deposited number of photons according to eq. 1, ΔN_P: Error in deposited number of photons, X: Conversion according to eq. 3, ΔX: Error in conversion according to eq. 5.

λ / nm	E_{pulse} / µJ	ΔE_{pulse} / µJ	t / s	T_λ	N_P / µmol	ΔN_P / µmol	X	ΔX
-	0	0	0		0	0	0.01	0.00
410	410	1020	97	85.13	107.06	10.18	0.05	0.01
420	420	978	63	85.24	105.29	6.78	0.06	0.01
440	440	931	31	85.36	105.15	3.50	0.04	0.01
460	460	892	19	85.41	105.39	2.24	0.04	0.01
480	480	844	25	85.43	104.09	3.08	0.03	0.00
500	500	818	22	85.44	105.10	2.83	0.02	0.00
520	520	787	29	85.45	105.16	3.88	0.02	0.00
540	540	757	41	85.45	105.05	5.69	0.01	0.00
560	560	728	41	85.45	104.77	5.90	0.01	0.00
580	580	706	57	85.45	105.23	8.50	0.01	0.00
600	600	687	52	85.45	105.93	8.02	0.01	0.00

Table S7. Conversion of **MeO-PEG-SPP** and **MeO-PEG-AP** after single-wavelength (480 nm for SPP, 420 nm for AP) irradiation in different aqueous solutions. *: Conversion value for pH=7 for **MeO-PEG-SPP** was obtained from **Table S1**. *pH*: pH value determined via pH sensor, X: Conversion according to eq. 3, ΔX: Error in conversion according to eq. 5.

pH	X_{SPP}	ΔX_{SPP}	X_{AP}	ΔX_{AP}
0	0.00	0.00	0.21	0.02
1	0.01	0.00	0.93	0.01
2	0.11	0.01	0.93	0.01
3	0.19	0.02	0.98	0.00
4	0.19	0.02	1.00	0.00
5	0.19	0.02	1.00	0.00
6	0.18	0.02	1.00	0.00
7*	0.51	0.04	-	-

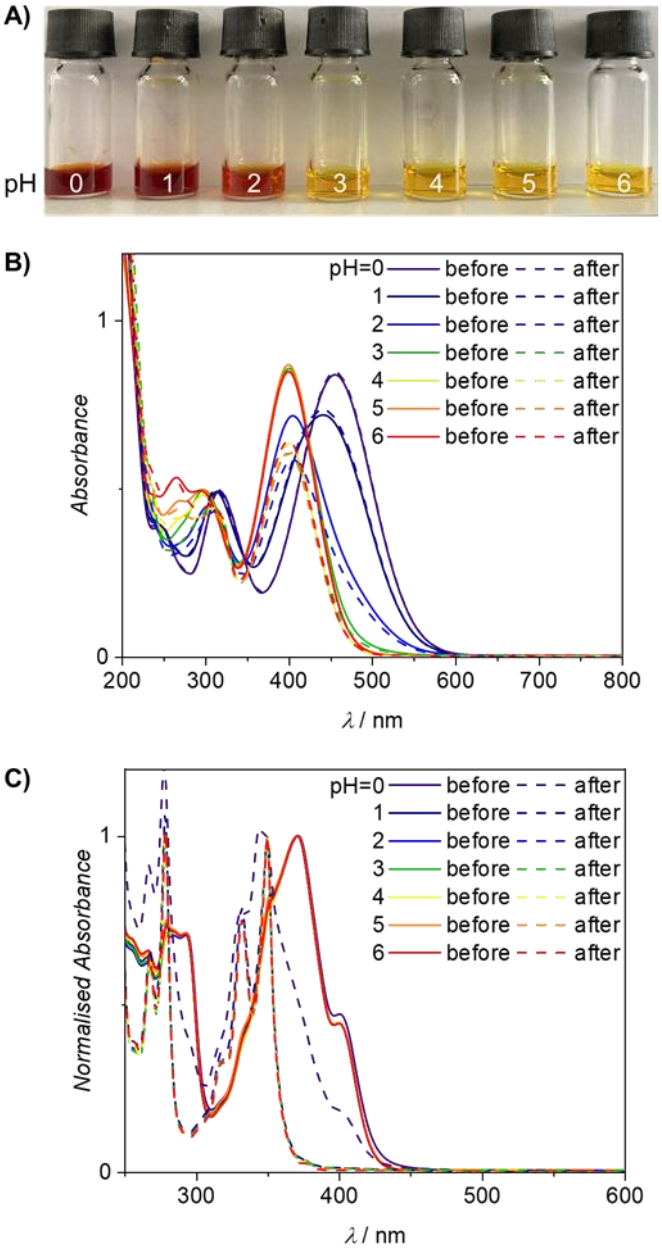

Figure S14. A) Image of **MeO-PEG-SPP** in water at different pH values. **B)** UV-Vis spectra of a solution of **MeO-PEG-SPP** at different pH before and after light irradiation (480 nm). **C)** UV-Vis spectra of a solution of **MeO-PEG-AP** at different pH before and after light irradiation (420 nm). All spectra were normalised to 371 nm before and 350 after irradiation.

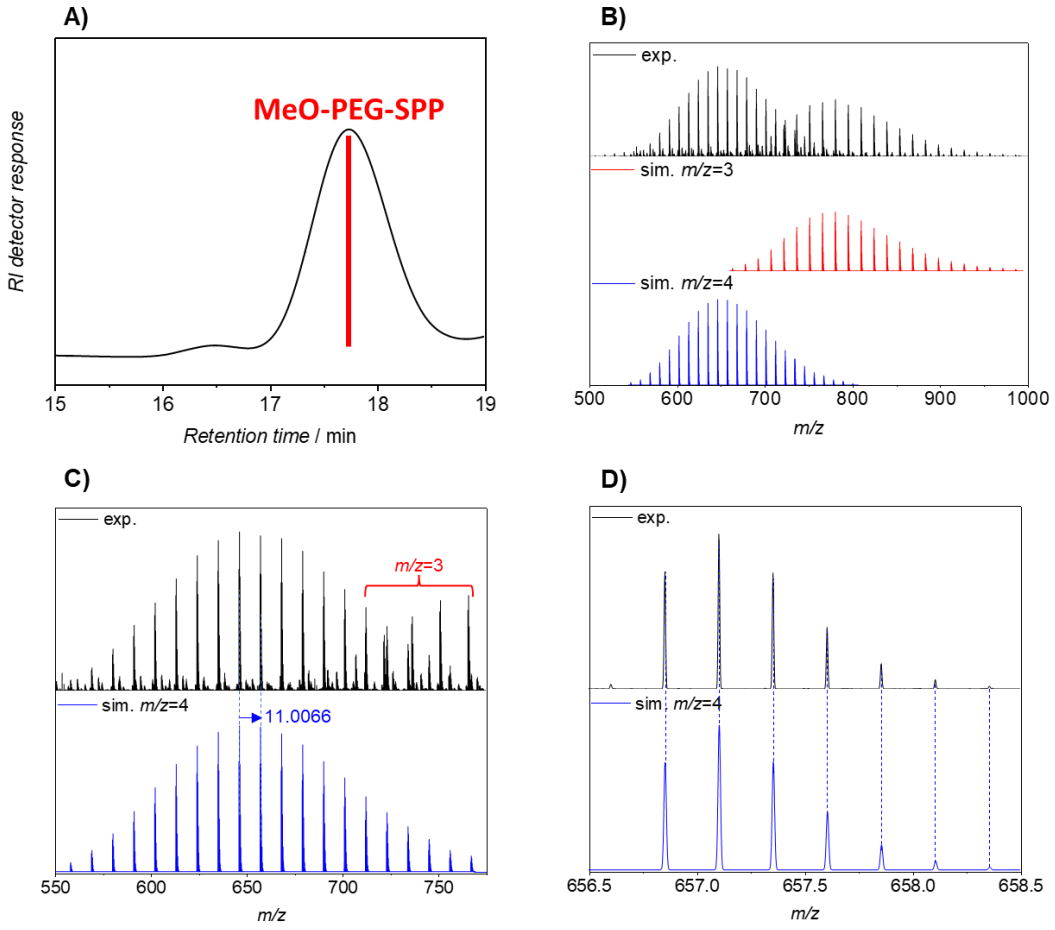

E)

Assignment	$m_{exp.}$	$m_{sim.}$	Δ / ppm	Composition
$[M+4Na]^{4+}$	657.1022	657.1034	1.83	$C_{119}H_{218}N_4O_{52}Na_4^{4+}$

Figure S15. A) Refractive Index (RI) SEC trace of **MeO-PEG-SPP** before irradiation. **B)** Extracted mass spectrum from the increment and assigned species with *m/z*=3 and m/z=4. **C)** Enlarged mass spectrum of the most abundant *z*=4 species and comparison with simulated isotopic data. **D)** Enlarged mass spectrum of the most abundant peak close to 657 and comparison with isotopic data. **E)** Assignment of the experimental mass of intact **MeO-PEG-SPP** to its simulation, alongside its derived error and composition.

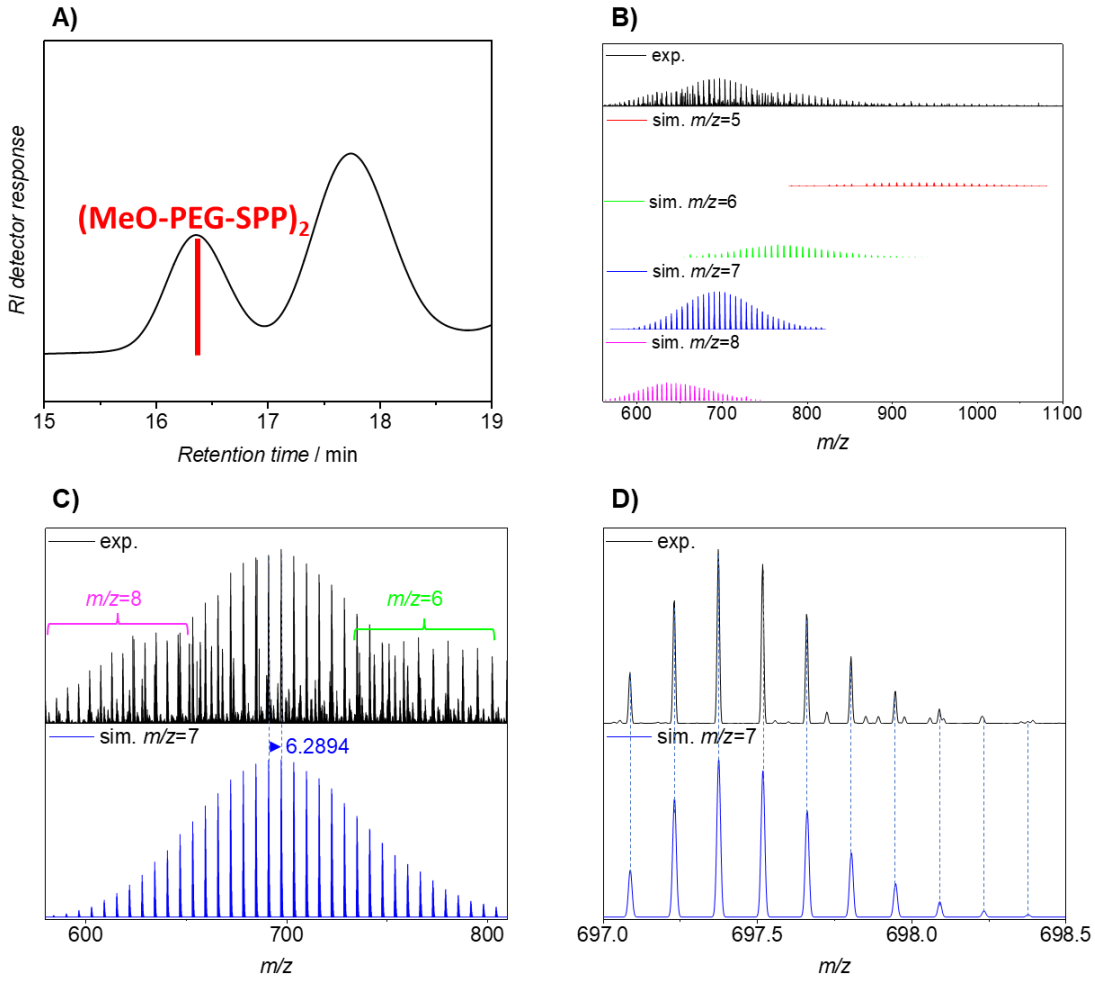

E)

Assignment	$m_{exp.}$	$m_{sim.}$	Δ / ppm	Composition
$[M+7Na]^{7+}$	697.3745	697.3756	1.58	$C_{222}H_{404}N_8O_{96}Na_7^{7+}$

Figure S16. A) Refractive Index (RI) SEC trace of **MeO-PEG-SPP** and **(MeO-PEG-SPP)$_2$** after irradiation. **B)** Extracted mass spectrum from the increment and assigned species between *m/z*=5 and *m/z*=9. **C)** Enlarged mass spectrum of the most abundant *z*=7 species and comparison with simulated isotopic distribution for the same species. **D)** Enlarged mass spectrum of the most abundant peak close to 698 and comparison with simulated isotopic distribution for the same species. **E)** Assignment of the experimental mass of intact **(MeO-PEG-SPP)$_2$** and theoretical mass, as well as its associated derived error and composition.

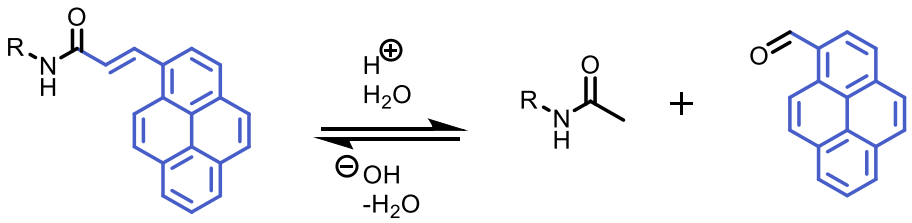

Scheme S2. Hydrolysis of the styryl moiety under acidic condition.

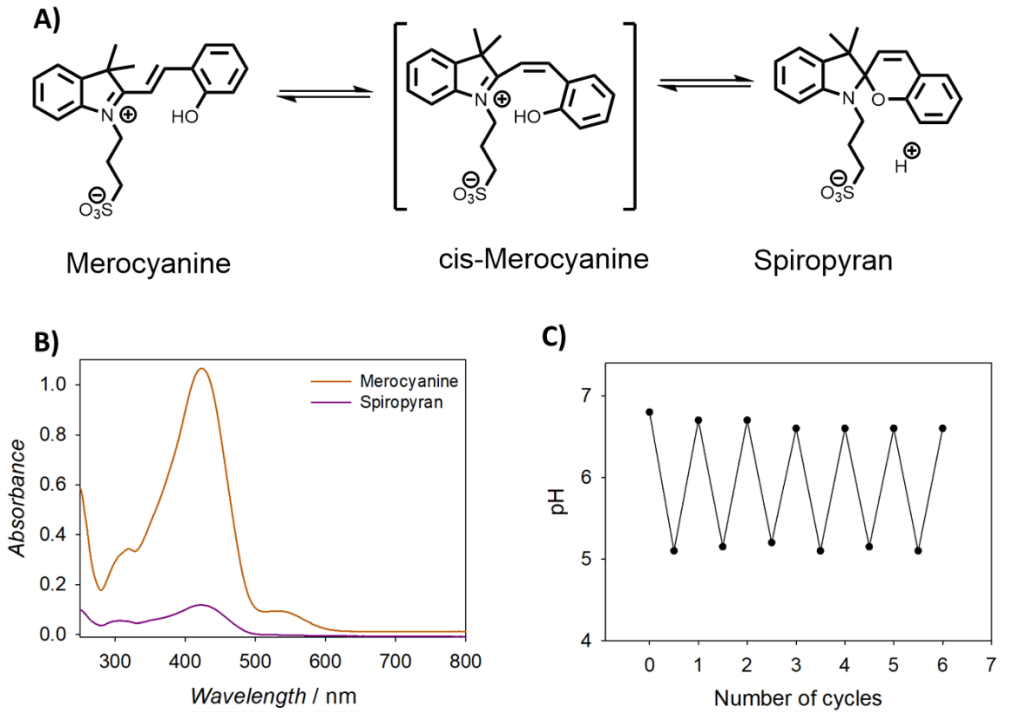

Figure S17. A) Photoswitching of the synthesized merocyanine PAG generator by visible light (400-510 nm) to its spiropyran form, releasing a proton during the process. The spiropyran form is rapidly reversed (in 5 min) to the merocyanine form in the dark. **B)** UV-vis absorbance spectra of the PAG in the merocyanine and spiropyran forms, respectively. **C)** The reversible switching of the PAG by light (at 445 nm, 2 min of irradiation) and in the dark (30 min) for up to 6 cycles in a solution having initial pH value of 6.8, displaying the changes in pH after each switch.

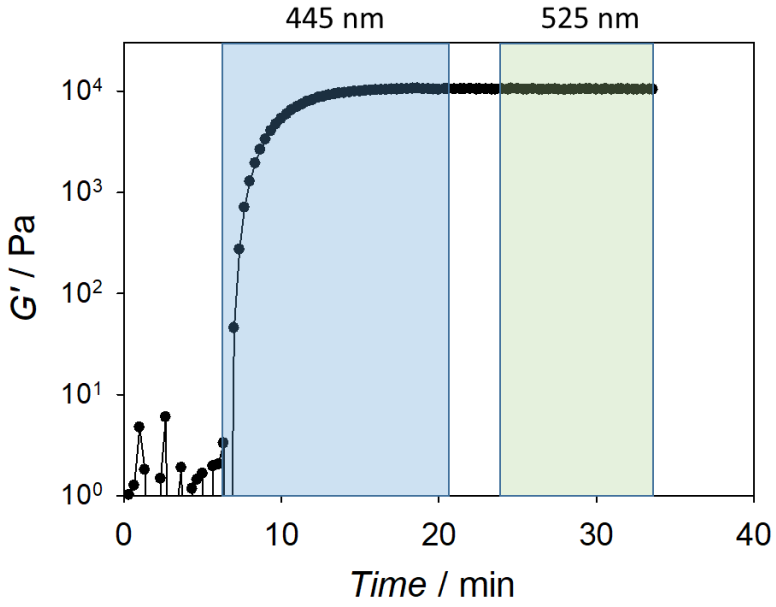

Figure S18. Rheology data of PEG-$(SPP)_3(AP)_4$ solution (5 mM) under irradiation of blue and green light (I = 20 mW cm^{-2}).

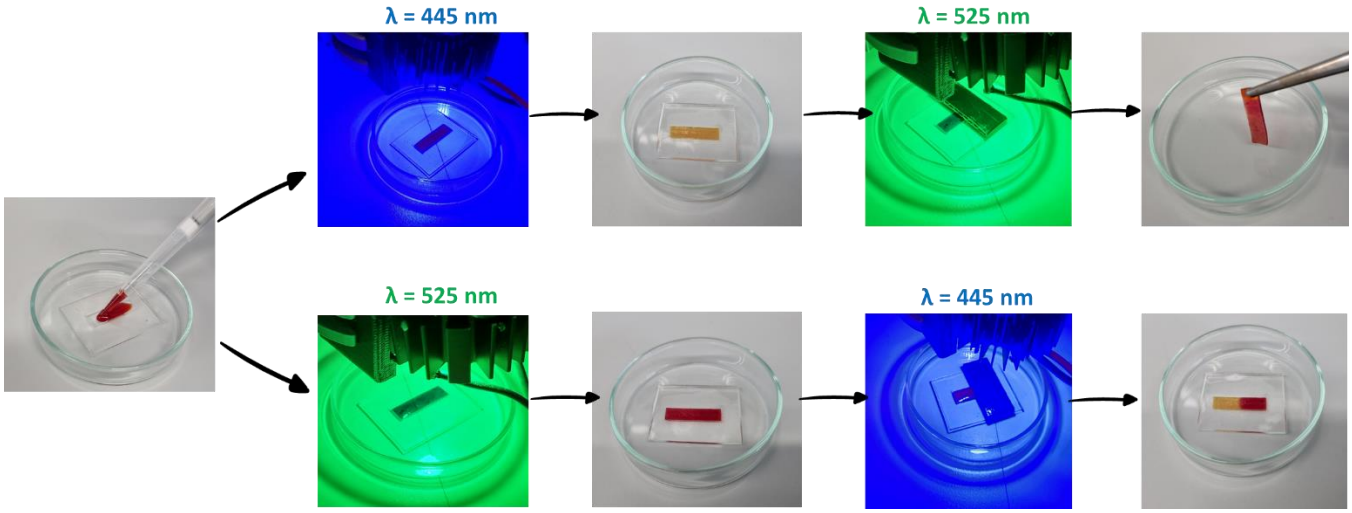

Figure S19. Photos of experiments demonstrating the spatial control over the crosslinking by different wavelengths of light. In the first experiment, hydrogel was from by irradiating the PEG-$(SPP)_3(AP)_4$ solution (10 wt%, ca. 4.7 mM) and PAG (0.5 mM) with blue light, during which the PAG was switched from its merocycanine form (red) to its spiropyran form (colourless), revealing the yellow colour of the AP and SPP dimer; irradiation of green light, partly covered by a mask, enabling the stiffening of the gel only on the irradiated part, during this time the spiropyran form was reverted back to the merocyanine form. In the second experiment, the gel was initially formed by irradiation with green light, causing no change to the merocyanine; blue light irradiation on the selected part of the gel triggered the second gelation and photobleaching of PAG.

References

[1] D. E. Fast, A. Lauer, J. P. Menzel, A.-M. Kelterer, G. Gescheidt, C. Barner-Kowollik, *Macromolecules* **2017**, *50*, 1815-1823.
[2] K. Kalayci, H. Frisch, V. X. Truong, C. Barner-Kowollik, *Nat. Commun* **2020**, *11*, 4193.
[3] M. Op de Beeck, A. Madder, *Journal of the American Chemical Society* **2012**, *134*, 10737-10740.
[4] B. T. Tuten, J. P. Menzel, K. Pahnke, J. P. Blinco, C. Barner-Kowollik, *Chemical Communications* **2017**, *53*, 4501-4504.
[5] K. De Bruycker, T. Krappitz, C. Barner-Kowollik, *ACS Macro Letters* **2018**, *7*, 1443-1447.
[6] K. Kalayci, H. Frisch, C. Barner-Kowollik, V. X. Truong, *Advanced Functional Materials* **2020**, *30*, 1908171.
[7] S. Shee, K. Ganguli, K. Jana, S. Kundu, *Chemcomm* **2018**, *54*, 6883-6886.